

## Rab7B/42 Is Functionally Involved in Protein Degradation on Melanosomes in Keratinocytes

Soujiro Marubashi and Mitsunori Fukuda\*

Laboratory of Membrane Trafficking Mechanisms, Department of Integrative Life Sciences, Graduate School of Life Sciences, Tohoku University, Aobayama, Aoba-ku, Sendai, Miyagi 980-8578, Japan

**ABSTRACT.** Keratinocytes uptake melanosomes from melanocytes and retain them in the perinuclear region, where they form melanin caps. Although these processes are crucial to protecting nuclear DNA against ultraviolet injury, the molecular basis of melanosome uptake and decomposition in keratinocytes is poorly understood. One of the major reasons for its being poorly understood is the lack of a specific marker protein that can be used to visualize or monitor melanosomes (or melanosome-containing compartments) that have been incorporated into keratinocytes. In this study, we performed a comprehensive localization screening for mammalian Rab family small GTPases (Rab1–45) and succeeded in identifying 11 Rabs that were enriched around melanosomes that had been incorporated into keratinocytes. We also established a new assay by using a recently developed melanosome probe (called M-INK) as a means of quantitatively assessing the degradation of proteins on incorporated melanosomes in control and each of a series of Rab-knockdown keratinocytes. The results showed that knockdown or CRISPR/Cas9-mediated knockout of Rab7B (also identified as Rab42) in keratinocytes caused strong inhibition of protein degradation on melanosomes. Our findings indicated that Rab7B/42 is recruited to melanosome-containing compartments and that it promotes protein degradation on melanosomes in keratinocytes.

**Key words:** degradation, keratinocytes, melanocytes, melanosome, Rab small GTPase

### Introduction

Melanosomes are specialized organelles that store melanin pigments in mammalian skin melanocytes (Raposo and Marks, 2007). Melanin is synthesized by melanogenic enzymes, e.g., tyrosinase and tyrosinase-related protein 1 (Typr1), and deposited within melanosomes. Mature darkly pigmented melanosomes are transported to the periphery of the melanocytes along the cytoskeleton, and they are ultimately transferred to surrounding keratinocytes (Boissy, 2003; Ohbayashi and Fukuda, 2012). After the melano-

somes have been incorporated into the keratinocytes, melanin forms supranuclear caps (called “melanin caps”) that protect nuclear DNA against ultraviolet injury (Kobayashi *et al.*, 1998). During the past few decades, a number of proteins involved in the biogenesis and transport of melanosomes in melanocytes have been identified (Ohbayashi and Fukuda, 2012; Bowman *et al.*, 2019), and their molecular mechanisms and functions have gradually been elucidated (Serre *et al.*, 2018). By contrast, the molecular mechanism of melanosome transfer from melanocytes to keratinocytes has remained elusive and is still a matter of controversy, although several transfer models and a related melanosome receptor have been proposed (Seiberg *et al.*, 2000; Ando *et al.*, 2012; Wu *et al.*, 2012; Tarafder *et al.*, 2014; and reviewed in Van Den Bossche *et al.*, 2006; and Tadokoro and Takahashi, 2017). Moreover, subsequent processes such as accumulation and decomposition of the incorporated melanosomes in keratinocytes are poorly understood.

Actually, there have been conflicting reports on the fate or final destination of the melanosomes incorporated into keratinocytes. Some studies have reported that the melanosomes are degraded by autophagy (Murase *et al.*, 2013; Yang *et al.*, 2018; Kim *et al.*, 2019), while others have

\*To whom correspondence should be addressed: Mitsunori Fukuda, Laboratory of Membrane Trafficking Mechanisms, Department of Integrative Life Sciences, Graduate School of Life Sciences, Tohoku University, Aobayama, Aoba-ku, Sendai, Miyagi 980-8578, Japan.

Tel: +81-22-795-7731, Fax: +81-22-795-7733

E-mail: nori@tohoku.ac.jp

Abbreviations: EEA1, early endosomal antigen 1; EGFP, enhanced green fluorescent protein; KD, knockdown; KO, knockout; LAMP1, lysosomal-associated membrane protein 1; LBPA, lysobisphosphatidic acid; LysoT, LysoTracker Red; mCherry, monomeric Cherry; M-INK, Melanosome-Interacting Kif1c-tail; PBS, phosphate-buffered saline; RFP, red fluorescent protein; siRNA, small interfering RNA; Typr1, tyrosinase-related protein 1.

reported that they reside in nondegradative compartments (Correia *et al.*, 2018; Hurbain *et al.*, 2018). Although several proteins (e.g., LAMP1 [lysosomal-associated membrane protein 1], CD63, EEA1 [early endosomal antigen 1], Rab5B, and LC3) have been observed in melanosome-containing compartments (Murase *et al.*, 2013; Hurbain *et al.*, 2018; Correia *et al.*, 2018), no specific marker protein for such compartments in keratinocytes has been identified, and no appropriate assay to assess the degradation of proteins on melanosomes in keratinocytes has been established.

In this study, we performed a comprehensive localization screening for mouse and human Rab family members (Matsui *et al.*, 2011; Ishida *et al.*, 2012), each of which is thought to localize to a specific membrane compartment(s) (or organelle[s]) and regulates its trafficking (Fukuda, 2008; Pfeffer, 2013; Stenmark, 2009), and succeeded in identifying 11 Rabs that were enriched around melanosomes that had been incorporated into keratinocytes. We then developed a new assay to quantitatively assess the degradation of proteins on such melanosomes in keratinocytes and found that depletion of Rab7B (also identified as Rab42; Itoh *et al.*, 2006; referred to as Rab7B/42 below) in keratinocytes resulted in the strongest inhibition of protein degradation on incorporated melanosomes. Our findings indicated that Rab7B/42 promotes protein degradation on melanosomes in keratinocytes.

## Materials and Methods

### Materials

Anti-Rab7B/42 rabbit polyclonal antibody was produced by using purified GST-tagged mouse Rab7B/42 as described previously (Azouz *et al.*, 2012; Homma *et al.*, 2019). Anti-tyrosinase rabbit polyclonal antibody was prepared as described previously (Beaumont *et al.*, 2011). The following antibodies used in this study were obtained commercially: anti-LAMP1 rat monoclonal antibody (clone: 1D4B) and anti-GM130 mouse monoclonal antibody (clone: 35) (BD Biosciences, San Jose, CA); anti-LBPA (lysobisphosphatidic acid; late endosome marker) mouse monoclonal antibody (clone: 6C4; Echelon Biosciences, Salt Lake City, UT); anti-EEA1 rabbit monoclonal antibody (clone: C45B10; Cell Signaling Technology, Danvers, MA); anti-LC3 rabbit monoclonal antibody (PM036; MBL, Nagoya, Japan); anti-Nogo-A mouse monoclonal antibody (AHP1799; Bio-Rad); anti-Pmel mouse monoclonal antibody (clone: HMB45) (Dako North America, Carpinteria, CA); anti-Tyrp1 mouse monoclonal antibody (clone: Ta99) and anti-Myc mouse monoclonal antibody (clone: 9E10) (Santa Cruz Biotechnology, Santa Cruz, CA); anti-Myc rabbit monoclonal antibody (C3956) and horseradish peroxidase-conjugated anti-FLAG tag (M2) mouse monoclonal antibody (Sigma-Aldrich, St. Louis, MO); anti-RFP (red fluorescent protein) rabbit monoclonal antibody (600-401-379; Rockland, Gil-

bertsville, PA), anti- $\beta$ -actin mouse monoclonal antibody (G043; Applied Biological Materials, Richmond, BC, Canada); and Alexa Fluor-labeled secondary antibodies (Thermo Fisher Scientific, Waltham, MA). All other reagents used in this study were analytical grade or the highest grade commercially available.

### Plasmids and small interfering RNAs (siRNAs)

pEGFP-C1 (Takara Bio Inc., Shiga, Japan) vectors carrying mouse Rab1A–43, pEF-FLAG-Rab7B/42, and pMRX-IRES-puro-EGFP-Rab7B/42 were prepared as described previously (Fukuda, 2003; Matsui *et al.*, 2011; Etoh and Fukuda, 2019). The mouse Rab44 and Rab45 cDNAs were amplified from the Marathon-Ready adult brain and testis cDNAs (Takara Bio Inc.) by using specific pairs of oligonucleotides (sequence information available upon request) as described previously (Fukuda, 2003) and then subcloned into the pEGFP-C1 vector. The Rab nomenclature in this study is the nomenclature used in the National Center for Biotechnology Information (NCBI) database, and thus the names of several Rabs, e.g., Rab7B (previously Rab42), Rab42 (previously Rab43), and Rab43 (previously Rab41), differ from the names used in Itoh *et al.* (2006). The M-INK cDNA (Ishida *et al.*, 2017) was subcloned into the pMRX-brs-Myc, pMRX-brs-EGFP, and pMRX-brs-mCherry vectors (Saitoh *et al.*, 2003) (a kind gift from Shoji Yamaoka, Tokyo Medical and Dental University, Tokyo, Japan). Effective siRNAs against mouse Rabs used in this study except *Rab44* siRNA (target sequence: 5'-GAGATCAGCTTGCT TTGA-3') were prepared as described previously (Matsui and Fukuda, 2013). The knockdown efficiency of these siRNAs was checked by co-expressing them with respective EGFP-tagged Rabs in cultured cells (Ishida *et al.*, 2012; Matsui and Fukuda, 2013; and data not shown).

### Cell cultures and transfections

Black-mouse-derived melanocyte cell line melan-a (a generous gift from Dorothy C. Bennett, St. George's Hospital Medical School, London, UK) (Bennett *et al.*, 1987) and mouse keratinocyte cell line XB2 (purchased from ATCC) were cultured as described previously (Ishida *et al.*, 2017). Plat-E cells (a kind gift from Toshio Kitamura, The University of Tokyo, Japan) and NIH3T3 cells were grown at 37°C in Dulbecco's modified Eagle medium (044-29765; FUJIFILM Wako Pure Chemical, Osaka, Japan) supplemented with 10% fetal bovine serum, 100 U/ml penicillin G, and 100  $\mu$ g/ml streptomycin in a 5% CO<sub>2</sub> incubator. An XB2 cell line stably expressing EGFP (enhanced green fluorescent protein)-Rab7B/42 or NIH3T3 cell lines stably expressing tagged (Myc, EGFP, or mCherry [monomeric Cherry])-M-INK were established by retrovirus infection as described previously (Morita *et al.*, 2000). Plasmids and siRNAs were transfected into XB2 cells by using Lipofectamine 2000 and Lipofectamine RNAiMAX (Thermo Fisher Scientific), respectively, each according to the manufacturer's protocol.

### **CRISPR/Cas9-mediated Rab7B/42 knockout (KO) in XB2 cells**

The CRISPR/Cas9-mediated Rab7B/42 KO [single guide RNA target sequence: 5'-TCAGGAGCGTTCCGCTCAA-3'] in XB2 cells was performed by using pSpCas9 (BB) 2A-Puro vector (ID# 80766; Addgene, Cambridge, MA) and the procedure described previously (Mrozowska and Fukuda, 2016). Clonal lines were isolated and analyzed by immunoblotting with anti-Rab7B/42 antibody to verify the loss of endogenous Rab7B/42 protein expression. *Rab7B/42* gene knockout was confirmed by sequencing genomic PCR products.

### **Preparation of melanosomes**

Confluent melan-a cells (one 10-cm dish) were scraped off the culture dish, homogenized in a homogenization buffer (0.25 M sucrose, 10 mM HEPES-KOH, pH 7.2, 1 mM 2-mercaptoethanol, and 1 mM EDTA) by passing them through a 27-gauge needle 5 times, and then centrifuged at 500×g for 1 minute. After collecting the supernatants and re-centrifuging at 10,000×g for 3 minutes, the pellets were washed twice with the homogenization buffer and centrifuged again at 10,000×g for 3 minutes. The pellets were then re-suspended in the homogenization buffer, frozen with liquid nitrogen, and stored at -80°C before use. The absorbance of the melanosome-rich solution was measured with a Bio-Photometer D30 (Eppendorf, Hamburg, Germany) at 340 nm, and the melanosome concentration was calculated according to a calibration curve developed in-house (absorbance=2.9876×concentration [μg/μl]-0.2854).

### **Preparation of M-INK-containing lysates**

Confluent M-INK-expressing NIH3T3 cells (one 10-cm dish) were scraped off the culture dish, homogenized in 1 ml of phosphate-buffered saline (PBS) by passing through a 27-gauge needle 3 times, and centrifuged at 17,000×g for 5 minutes. The supernatants were collected and used as M-INK-containing lysates (simply referred to as M-INK lysates below). The M-INK lysates were frozen with liquid nitrogen and stored at -80°C before use.

### **Uptake of melanosomes by keratinocytes**

XB2 cells were cultured on 24-well plates containing a 15-mm diameter coverslip, and 50 μg of purified melanosomes were added per 500 μl of culture medium. After incubation for 48 hours, the cells were fixed with 4% paraformaldehyde. The coverslips were incubated with a 100 μl volume of M-INK lysates (containing complete EDTA-free protease inhibitor cocktail [Roche Applied Science, Penzberg, Germany] and 0.05% saponin), then with primary antibodies and lastly with appropriate Alexa Fluor-conjugated secondary antibodies. The samples were mounted using ProLong Diamond Antifade Mountant (Thermo Fisher Scientific) and examined for fluorescence with a confocal fluorescence microscope (FV1000D, Olympus, Tokyo, Japan).

### **M-INK degradation assay**

Purified melanosomes were mixed with M-INK lysate (melanosome:M-INK lysate=1 μg:1 μl), incubated for 10 minutes, and then centrifuged at 10,000×g for 1 minute. The pellets were re-suspended with the culture medium and used immediately as M-INK-labeled melanosomes. After culturing XB2 cells with M-INK-labeled melanosomes, the cells were washed twice with PBS, collected by trypsinization, and centrifuged at 500×g for 1 minute. The cell pellets were lysed in an SDS sample buffer (62.5 mM Tris-HCl pH 6.8, 2% 2-mercaptoethanol, 10% glycerol, and 0.02% Bromophenol Blue) and boiled. The lysates were subjected to SDS-PAGE and transferred to a polyvinylidene difluoride membrane (Merck Millipore, Burlington, MA) by electroblotting. The blots were blocked with 5% skim milk in PBS containing 0.1% Tween-20 (FUJIFILM Wako Pure Chemical), incubated at room temperature with primary antibodies for 1 hour and then with appropriate horseradish peroxidase-conjugated secondary antibodies for 1 hour. Immunoreactive bands were detected by using the ChemiDoc Touch imaging system (Bio-Rad, Hercules, CA) and quantified with ImageJ software (version 1.52b; National Institutes of Health).

### **Assay for degradation of melanosomal proteins in keratinocytes**

XB2 cells were cultured on a 10-cm dish (or 6-cm dish for Fig. S4) with or without 1 mg of purified melanosomes. After incubation for 36 hours, the cells were washed twice with PBS, collected by trypsinization, and centrifuged at 500×g for 1 minute. The cell pellets were suspended in the homogenization buffer (containing complete EDTA-free protease inhibitor cocktail), homogenized by passing them through a 27-gauge needle 30 times, and then centrifuged at 3000×g for 5 minutes. The pellets were lysed in the SDS sample buffer, vortexed with 0.5 mm glass beads for 30 minutes at 4°C, and boiled for 15 minutes. The lysates obtained were analyzed by immunoblotting with anti-tyrosinase antibody and anti-Pmel antibody.

### **Live-cell imaging**

Live-cell fluorescence imaging was performed by using a FV1000D confocal fluorescence microscope with a 100×oil/1.4 NA Plan Apochromatic objective lens and Fluoview software. XB2 cells stably expressing EGFP-Rab7B/42 were placed on a 35-mm glass bottom dish (MatTek, Ashland, MA) and incubated for 2 hours with mCherry-M-INK-labeled melanosomes before imaging. During live-cell imaging, the dish was mounted in a chamber (INUB-ONI-F2; Tokai Hit Co., Ltd., Shizuoka, Japan) to maintain incubation conditions at 37°C and 5% CO<sub>2</sub>. Images were acquired at intervals of 10 minutes and analyzed with ImageJ software.

## Melanin assay

Melanin content was assayed as described previously (Tamura *et al.*, 2009). In brief, XB2 cells were cultured for 48 hours with melanosomes, washed two times with PBS, then cultured for 2 weeks in the absence of melanosomes. Their melanin content normalized to protein content was measured as optical density at 490 nm.

## Results

### **Melanosomes incorporated into keratinocytes are surrounded by LAMP1-positive and LysoTracker-negative structures**

To identify a membrane compartment containing melanosomes in mouse XB2 keratinocytes, we co-stained XB2 cells that had been cultured with isolated melanosomes for 48 hours for various organelle markers and melanosomes. We stained for melanosomes by using the recently developed M-INK (Melanocore-INTERacting Kif1c-tail) probe, which enables visualization of melanosomes in a fluorescent field (Ishida *et al.*, 2017). Fluorescence visualization with M-INK is more accurate in the z-axis direction than bright-field observation, and M-INK makes it possible to correctly determine the intracellular position of melanosomes that have been incorporated into keratinocytes. Conventional markers for melanosomes (e.g., tyrosinase and Tyrp1) in melanocytes cannot be used, because they are not stained in keratinocytes that have incorporated melanosomes (Fig. 1C; Ishida *et al.*, 2017). The results of the co-staining analysis showed that many of the melanosomes were surrounded by LAMP1-positive structures (Fig. 1A), but they were not well colocalized with other organelle markers, including EEA1 (early endosome marker), LBPA, LysoTracker Red (LysoT; lysosome marker), LC3 (autophagosome marker) and Nogo-A (ER marker) (Supplemental Fig. S1). Because LAMP1 is known to localize both in lysosomes and late endosomes (Humphries *et al.*, 2011), we also co-stained XB2 cells for LAMP1, LBPA (or LysoTracker Red), and melanosomes. Intriguingly, no M-INK-positive, LAMP1-positive structures were co-localized with LysoTracker Red or LBPA (Fig. 1B, arrowheads). Such LAMP1-positive, LysoTracker-negative localization of melanosomes in keratinocytes has also recently been described in another study (Correia *et al.*, 2018; Hurbain *et al.*, 2018). These findings indicated that the melanosomes in keratinocytes are present in a subset of LAMP1-positive structures that are different from both highly acidic, degradative lysosomes (i.e., LysoTracker-positive lysosomes) and conventional late endosomes (i.e., LBPA-positive late endosomes).

To further characterize the LAMP1-positive structures around the incorporated melanosomes, we focused on the

Rab family small GTPases, because approximately 60 different isoforms are present in mammals and each member is thought to localize to a specific membrane compartment(s) or organelle(s) (Fukuda, 2008; Pfeffer, 2013; Stenmark, 2009). We expressed each of 62 different EGFP-tagged Rabs (Rab1A–45) (Matsui *et al.*, 2011; Ishida *et al.*, 2012) in XB2 cells, and the incorporated melanosomes were visualized with M-INK. The results of a comprehensive Rab localization screening revealed that 11 Rabs, i.e., Rab7B/42, 19, 25, 27A, 27B, 32, 33A, 37, 38, 39A, and 44, were enriched around the incorporated melanosomes (Fig. 2) and that none of the other Rabs were localized around them (Supplemental Fig. S2). Intriguingly, neither early endosomal Rab5B, which has previously been shown to regulate melanosome uptake in keratinocytes (Correia *et al.*, 2018), late endosomal/lysosomal Rab7A, which is involved in the degradation of endocytosed receptors (Guerra and Bucci, 2016), nor recycling endosomal Rab11B, which is required for melanosome transfer from melanocytes to keratinocytes (Tarafder *et al.*, 2014), was among the 11 candidate Rabs identified by screening. We therefore speculated that melanosomes that have been incorporated into keratinocytes are present in an as yet unidentified Rab-positive, LAMP1-positive compartment.

### **An incorporated-melanosome-containing structure is a degradative compartment: establishment of an assay for M-INK degradation in keratinocytes**

Although no incorporated melanosomes were detected in LysoTracker-positive lysosomes (Fig. 1B), Tyrp1 signals largely disappeared when melanosomes were incorporated into XB2 cells (Fig. 1C, upper insets), suggesting that the incorporated-melanosome-containing structures in keratinocytes still had degradative activity. Because melanogenic enzymes such as tyrosinase and Tyrp1 are rapidly degraded in keratinocytes (Ishida *et al.*, 2017), it is extremely difficult to monitor their degradation over a long period. To overcome this problem, we developed an M-INK degradation assay (see Materials and Methods for details) in order to be able to quantitatively assess protein degradation on melanosomes in keratinocytes. In brief, we pre-labeled melanosomes with mCherry-M-INK, incorporated them into keratinocytes, and then detected the mCherry-M-INK in the keratinocytes by immunoblotting with anti-RFP antibody. Although the amount of full-length incorporated mCherry-M-INK was much lower (Fig. 3A; compare lanes 1 and 2; ~60 kDa band), the mCherry band itself seemed to have been protected even after incubating the melanosomes in XB2 cells for 24 hours (Fig. 3A; ~30 kDa band), presumably because mCherry is less susceptible to degradation than M-INK is. It should be noted that the degradation of M-INK was almost completely inhibited by treatment with the protease inhibitors E64d and pepstatin A (Fig. 3A, lane 3). We therefore decided to use the ratio of mCherry-M-

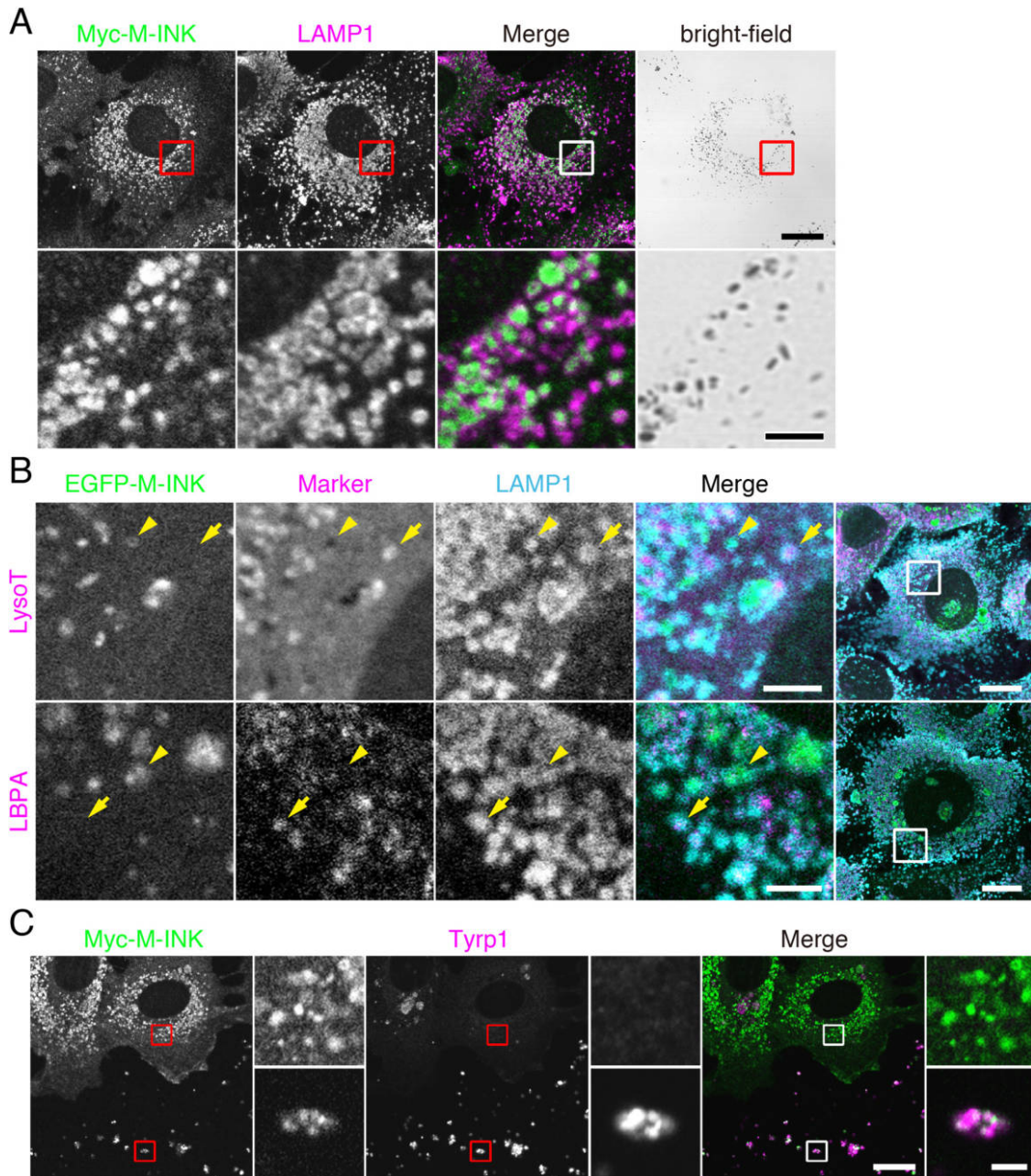


**Fig. 1.** Melanosomes incorporated by keratinocytes are surrounded by LAMP1-positive structures. XB2 cells were cultured with melanosomes for 48 hours. (A) The cells were stained for Myc-M-INK (green) and LAMP1 (magenta). (B) LysoTracker Red (LysoT) was added 15 minutes before fixation. The cells were stained for EGFP-M-INK (green), LBPAs (magenta), and LAMP1 (cyan). The arrowheads point to structures positive for both M-INK and LAMP1. The arrows point to M-INK-negative, LAMP1-positive structures. (C) The cells were stained for Myc-M-INK (green) and Tyrp1 (magenta). Upper insets, Tyrp1-negative melanosomes in keratinocytes; and lower insets, Tyrp1-positive extracellular melanosomes. Scale bars=15 μm (3 μm in magnified views of A and B, and 2 μm in magnified views of C).

INK to mCherry as an index of melanosomal protein degradation, and we succeeded in quantitatively comparing the degradation of mCherry-M-INK in the presence and absence of protease inhibitors (Fig. 3B).

We used our assay to investigate the candidate Rabs that surrounded the incorporated melanosomes (Fig. 2) for involvement in protein degradation on melanosomes. We knocked down each candidate Rab in XB2 cells with spe-

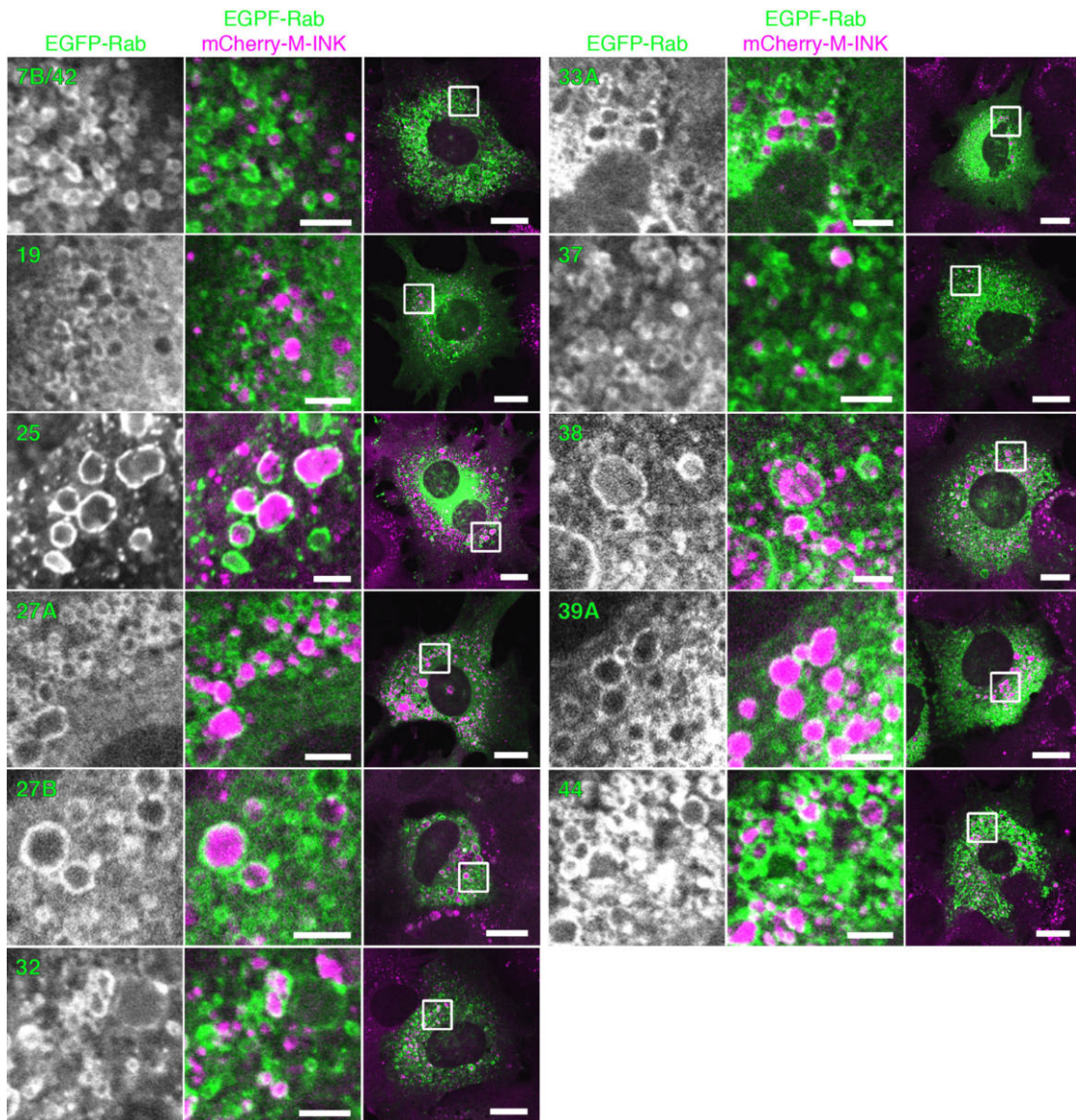


**Fig. 2.** Rabs that are specifically localized around melanosomes incorporated into keratinocytes. XB2 cells expressing EGFP-Rabs (Rab1A–45; green) were stained for mCherry-M-INK (magenta). Only 11 of the Rabs were enriched around the incorporated melanosomes, and none of the other Rabs were localized around the incorporated melanosomes (see Supplemental Fig. S2). Scale bars=15  $\mu$ m (3  $\mu$ m in magnified views).

cific siRNAs (Matsui and Fukuda, 2013) and evaluated the degradation ability of each Rab-knockdown (KD) cells. The results showed that knockdown of Rab7B/42 most strongly and significantly inhibited M-INK degradation (Fig. 3C and D). Rab7B/42 has previously been reported to be localized at different organelles in other cell types, e.g., at late endosomes or the *trans*-Golgi network (TGN) in HeLa cells (Progida *et al.*, 2010; Progida *et al.*, 2012) and late endosomes or lysosomes in immune cells (Yang *et al.*, 2004; Wang *et al.*, 2007; Yao *et al.*, 2009), and to be impli-

cated in the trafficking and degradation of certain immune receptors (Wang *et al.*, 2007; Yao *et al.*, 2009), cathepsin-D maturation (Progida *et al.*, 2010), and autophagy (Kjos *et al.*, 2017). Based on these previous observations together with our own finding that Rab7B/42 is strongly colocalized with LAMP1 but weakly colocalized with LysoTracker Red or LBPA in XB2 cells (Supplemental Fig. S3), we selected Rab7B/42 as the prime candidate for subsequent analysis as the Rab that regulates protein degradation on melanosomes.

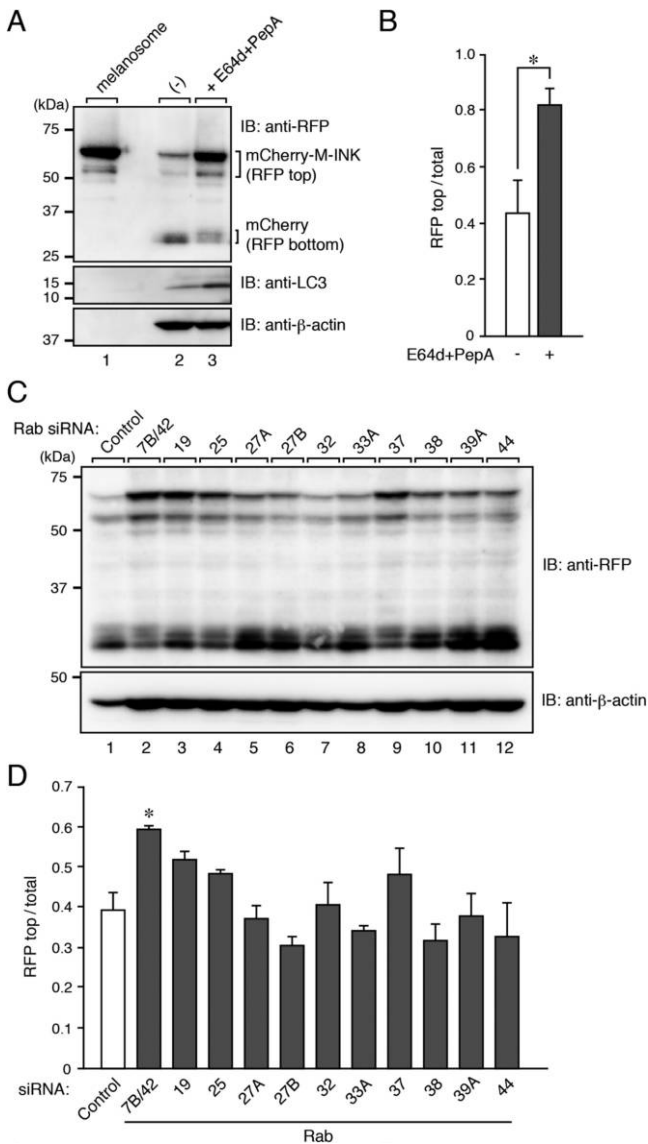


**Fig. 3.** Degradation of M-INK in Rab-KD XB2 cells. (A) XB2 cells were cultured with mCherry-M-INK-labeled melanosomes for 24 hours in the presence or absence of E64d and pepstatin A and assessed for degradation of M-INK by immunoblotting. (B) Quantification of RFP-positive bands shown in the top panel in A. The total amount of RFP/mCherry was calculated by adding the top and bottom RFP-positive bands (mean+s.e.m.; n=3). \*,  $p < 0.05$  (Student's unpaired *t* test). (C) XB2 cells were treated with control or Rab siRNAs and then cultured with mCherry-M-INK-labeled melanosomes for 24 hours. The cell lysates were analyzed by immunoblotting. (D) Quantification of RFP-positive bands shown in the top panel in C (mean+s.e.m.; n=3). \*,  $p < 0.05$  compared with the control (Dunnett's test).

**Rab7B/42 promotes protein degradation on melanosomes in keratinocytes**

To investigate the timing and position of Rab7B/42 recruitment to melanosomes in keratinocytes in greater detail, we

performed live-cell imaging of XB2 cells stably expressing EGFP-Rab7B/42 in the presence of mCherry-M-INK-labeled melanosomes. Examination of serial section images revealed that EGFP-Rab7B/42 gradually accumulated around the melanosomes (Fig. 4, arrows and arrowheads; and Supplemental Movies 1 and 2).

We then generated a Rab7B/42-KO cell line by using the CRISPR/Cas9 system, and we succeeded in confirming the loss of its protein by immunoblotting with specific antibody (Fig. 5A). To evaluate the degradation ability of Rab7B/42-KO cells, we incubated the cells with mCherry-M-INK-labeled melanosomes and investigated the degradation of mCherry-M-INK by immunoblotting with anti-RFP antibody as described in Fig. 3A. Consistent with the results of Rab7B/42 KD shown in Fig. 3D, Rab7B/42 KO caused a significant and clear delay of protein degradation on the melanosomes in the keratinocytes (Fig. 5B and C). Moreover, the inhibition of M-INK degradation in the absence of Rab7B/42 was clearly rescued by re-expression of Rab7B/42 in Rab7B/42-KO cells (Fig. 5D and E).

Finally, we evaluated the degradation of endogenous melanosomal proteins, i.e., tyrosinase and Pmel (also called Pmel17/gp100), in parental and Rab7B/42-KO cells by incubating the cells with or without melanosomes. The results showed that Rab7B/42 KO significantly inhibited the degradation of the two melanosomal proteins (Fig. 6), consistent with the impaired M-INK degradation shown in Fig. 5. Such inhibitory effects are unlikely to be caused by clonal variations of XB2 cells, because inhibition of tyrosinase and Pmel degradation was also observed in another independent Rab7B/42 KO#2 clone and because it was clearly rescued by re-expression of Rab7B/42 (Supplemental Fig. S4). These results indicated that Rab7B/42 promotes protein degradation on melanosomes in keratinocytes.

**Discussion**

In the present study, we used a collection of EGFP-tagged Rabs together with an M-INK probe and succeeded in demonstrating that melanosomes that have been incorporated into mouse XB2 keratinocytes are surrounded by structures that are LAMP1- and Rab7B/42-positive, but LysoTracker-negative (Fig. 1, Fig. 2, and Fig. 4). We also found that depletion of Rab7B/42 in XB2 cells caused strong inhibition of protein degradation on incorporated melanosomes (Fig. 3, Fig. 5, and Fig. 6), but that M-INK degradation in Rab7B/42-KO cells was not completely blocked (Fig. 5C, 36 hours). This residual degradation activity may be mediated by other Rab isoforms that are also present around melanosomes. Actually, our screening procedure identified 10 additional Rabs (i.e., Rab19, 25, 27A, 27B, 32, 33A, 37, 38, 39A, and 44), and some of them have been shown to be involved in related processes in other cell types; e.g.,

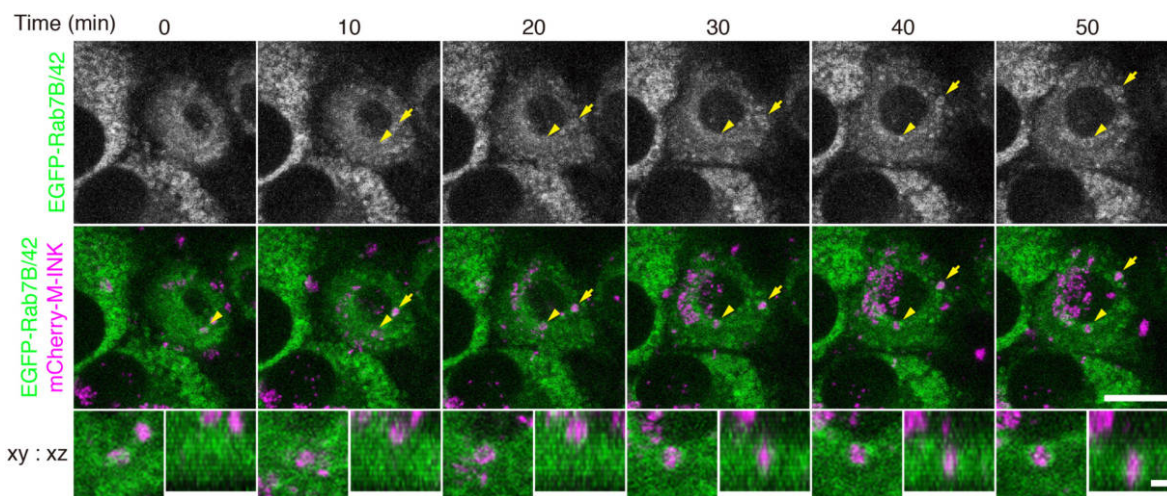


**Fig. 4.** EGFP-Rab7B/42 accumulates around melanosomes incorporated into keratinocytes. Live imaging of EGFP-Rab7B/42 stably expressing in XB2 cells after adding mCherry-M-INK-labeled melanosomes. The images were stacked by z-projection. The arrowheads and arrows point to EGFP-Rab7B/42 accumulations around incorporated melanosomes (see also Supplemental Movies 1 and 2). Magnified views are stacked images of the incorporated melanosomes pointed to the arrowheads. Scale bars=15  $\mu\text{m}$  (2  $\mu\text{m}$  in magnified views).

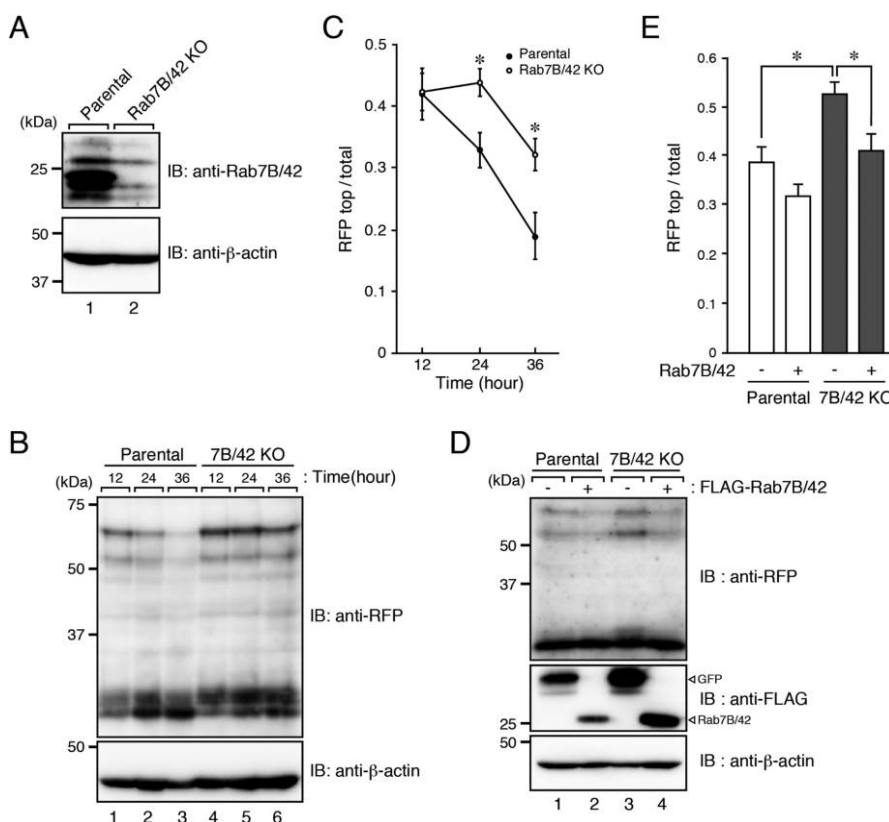


**Fig. 5.** Impaired M-INK degradation in Rab7B/42-KO XB2 cells. (A) Expression of Rab7B/42 in parental and Rab7B/42-KO XB2 cells. (B) Parental and Rab7B/42-KO cells were incubated for 12 hours with mCherry-M-INK-labeled melanosomes and then cultured for the times indicated in the absence of melanosomes. The cell lysates were analyzed by immunoblotting. (C) Quantification of RFP-positive bands shown in the top panel in B (mean+s.e.m.; n=3). \*,  $p < 0.05$  (Student's unpaired  $t$  test). (D) Parental and Rab7B/42-KO cells expressing FLAG-Rab7B/42 (or FLAG-GFP) were cultured with mCherry-M-INK-labeled melanosomes for 24 hours, and immunoblotting was performed. (E) Quantification of RFP-positive bands shown in the top panel in D (mean+s.e.m.; n=10). \*,  $p < 0.05$  (Tukey's test).



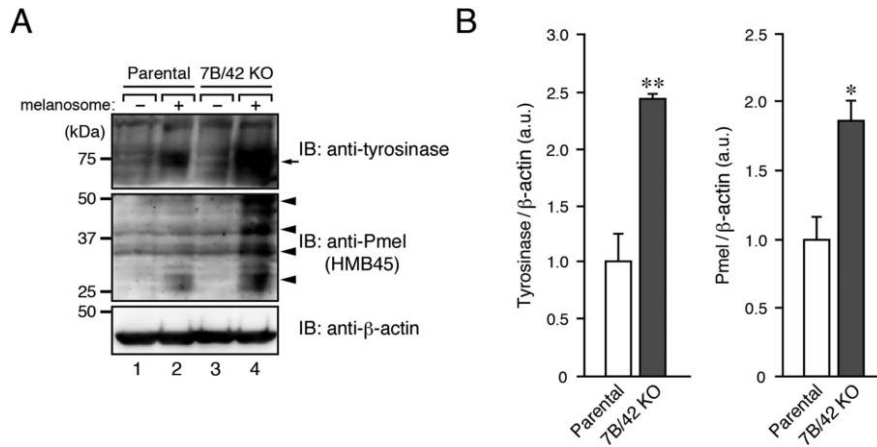


**Fig. 6.** Rab7B/42-KO in keratinocytes inhibits melanosomal protein degradation. (A) Parental and Rab7B/42-KO cells were incubated for 36 hours with or without melanosomes. The lysates of the melanosome-containing compartment or the total cell lysates (for  $\beta$ -actin) were analyzed by immunoblotting with the antibodies indicated. (B) Quantification of tyrosinase (arrow) and Pmel bands (arrowheads) shown in the top and middle panels, respectively, in A (mean $\pm$ s.e.m.; n=3). \*,  $p < 0.05$ ; \*\*,  $p < 0.01$  (Student's unpaired *t* test).

Rab27A and Rab32 have been shown to be recruited around internalized pathogens and involved in subsequent clearance processes (Yokoyama *et al.*, 2011; Spanò *et al.*, 2016). Further research will be necessary to determine the function of these Rabs in the uptake, transport, and/or decomposition of melanosomes in keratinocytes. Intriguingly, two well-known Rabs, Rab5B, which regulates melanosome uptake in keratinocytes (Correia *et al.*, 2018), and Rab7A, which generally regulates the endocytic pathway (Guerra and Bucci, 2016), were not identified by our screening procedure (Supplemental Fig. S2). The absence of Rab5B in the candidate list is probably attributable to having imaged keratinocytes 48 hours after the addition of melanosomes, which is much later than the time when melanosome uptake occurs. Although Rab7B is the closest isoform of Rab7A, Rab7A itself is not recruited around incorporated melanosomes and is unlikely to play a major role in protein degradation on melanosomes, suggesting the existence of functional diversity between two Rab7 isoforms in keratinocytes.

How does Rab7B/42 promote protein degradation on melanosomes in keratinocytes? Because Rab7B/42 has been shown to be involved in cathepsin-D maturation (Progida *et al.*, 2010) and Rab7B/42 is well colocalized with LAMP1 in keratinocytes (Supplemental Fig. S3), Rab7B/42 is likely to regulate the trafficking of certain E64d- and pepstatin A-sensitive proteases to LAMP1-positive, LysoTracker-negative compartments. Identification of proteases that degrade proteins on melanosomes at relatively higher pH's, at which LysoTracker is negative, is an important task that needs to be addressed in a future study. Although the Rab7B/42-positive melanosome-containing compartments identified in our study have the ability to degrade proteins on melanosomes (e.g., tyrosinase

and Pmel; Fig. 6 and Supplemental Fig. S4), no melanin itself had been degraded in either parental or Rab7B/42-KO cells even after two weeks (Supplemental Fig. S5), suggesting that melanin degradation occurs in a compartment(s) other than Rab7B/42- and LAMP1-positive compartments. One possible degradation mechanism is autophagy, but LC3 was not well colocalized with the incorporated melanosomes in our study (Supplemental Fig. S1). However, since the presence of LC3 has been reported in the upper layers of the epidermis (Akinduro *et al.*, 2016; Hurbain *et al.*, 2018), keratinocyte differentiation may regulate autophagic activity and promote melanin degradation.

In conclusion, we have demonstrated that incorporated melanosomes are present in Rab7B/42- and LAMP1-positive compartments and that Rab7B/42 can promote protein degradation on melanosomes without altering the melanin content of keratinocytes. Our findings provide new insights into the degradation processes of melanosomes in keratinocytes, and the M-INK degradation assay developed in this study will be useful in analyzing the precise molecular mechanism of protein degradation on melanosomes in the future.

*Acknowledgments.* We thank Drs. Dorothy C Bennett, Toshio Kitamura, and Shoji Yamaoka for kindly donating materials, Megumi Takada-Aizawa and Kazuyasu Shoji for technical assistance, Morié Ishida for initial M-INK experiments, and members of the Fukuda laboratory for valuable discussions. This work was supported in part by Grant-in-Aid for Scientific Research(B) from the MEXT (grant number 19H03220 to MF), by Japan Science and Technology Agency (JST) CREST (grant Number JPMJCR17H4 to MF), by a grant from the Hoyu Science Foundation (to MF), by a grant from the Kao Melanin Workshop (to SM), by the Japan Society for the Promotion of Science (to SM), and by Tohoku University Division for interdisciplinary Advanced Research and Education (to SM).

## References

- Akinduro, O., Sully, K., Patel, A., Robinson, D.J., Chikh, A., McPhail, G., Braun, K.M., Philpott, M.P., Harwood, C.A., Byrne, C., O'Shaughnessy, R.F.L., and Bergamaschi, D. 2016. Constitutive autophagy and nucleophagy during epidermal differentiation. *J. Invest. Dermatol.*, **136**: 1460–1470.
- Ando, H., Niki, Y., Ito, M., Akiyama, K., Matsui, M.S., Yarosh, D.B., and Ichihashi, M. 2012. Melanosomes are transferred from melanocytes to keratinocytes through the processes of packaging, release, uptake, and dispersion. *J. Invest. Dermatol.*, **132**: 1222–1229.
- Azouz, N.P., Matsui, T., Fukuda, M., and Sagi-Eisenberg, R. 2012. Decoding the regulation of mast cell exocytosis by networks of Rab GTPases. *J. Immunol.*, **189**: 2169–2180.
- Beaumont, K.A., Hamilton, N.A., Moores, M.T., Brown, D.L., Ohbayashi, N., Cairncross, O., Cook, A.L., Smith, A.G., Misaki, R., Fukuda, M., Taguchi, T., Sturm, R.A., and Stow, J.L. 2011. The recycling endosome protein Rab17 regulates melanocytic filopodia formation and melanosome trafficking. *Traffic*, **12**: 627–643.
- Bennett, D.C., Cooper, P.J., and Hart, I.R. 1987. A line of non-tumorigenic mouse melanocytes, syngeneic with the B16 melanoma and requiring a tumour promoter for growth. *Int. J. Cancer*, **39**: 414–418.
- Boissy, R.E. 2003. Melanosome transfer to and translocation in the keratinocyte. *Exp. Dermatol.*, **12**: 5–12.
- Bowman, S.L., Bi-Karchin, J., Le, L., and Marks, M.S. 2019. The road to lysosome-related organelles: insights from Hermansky-Pudlak syndrome and other rare diseases. *Traffic*, **20**: 404–435.
- Correia, M.S., Moreiras, H., Pereira, F.J.C., Neto, M.V., Festas, T.C., Tarafder, A.K., Ramalho, J.S., Seabra, M.C., and Barral, D.C. 2018. Melanin transferred to keratinocytes resides in nondegradative endocytic compartments. *J. Invest. Dermatol.*, **138**: 637–646.
- Etoh, K. and Fukuda, M. 2019. Rab10 regulates tubular endosome formation through KIF13A and KIF13B motors. *J. Cell Sci.*, **132**: jcs226977.
- Fukuda, M. 2003. Distinct Rab binding specificity of Rim1, Rim2, raphilin, and Noc2: identification of a critical determinant of Rab3A/Rab27A recognition by Rim2. *J. Biol. Chem.*, **278**: 15373–15380.
- Fukuda, M. 2008. Regulation of secretory vesicle traffic by Rab small GTPases. *Cell. Mol. Life Sci.*, **65**: 2801–2813.
- Guerra, F. and Bucci, C. 2016. Multiple roles of the small GTPase Rab7. *Cells*, **5**: 34.
- Homma, Y., Kinoshita, R., Kuchitsu, Y., Wawro, P.S., Marubashi, S., Oguchi, M.E., Ishida, M., Fujita, N., and Fukuda, M. 2019. Comprehensive knockout analysis of the Rab family GTPases in epithelial cells. *J. Cell Biol.*, **218**: 2035–2050.
- Humphries, W.H., IV, Szymanski, C.J., and Payne, C.K. 2011. Endolysosomal vesicles positive for Rab7 and LAMP1 are terminal vesicles for the transport of dextran. *PLoS One*, **6**: e26626.
- Hurbain, I., Romao, M., Sextius, P., Bourreau, E., Marchal, C., Bernerd, F., Duval, C., and Raposo, G. 2018. Melanosome distribution in keratinocytes in different skin types: melanosome clusters are not degradative organelles. *J. Invest. Dermatol.*, **138**: 647–656.
- Ishida, M., Ohbayashi, N., Maruta, Y., Ebata, Y., and Fukuda, M. 2012. Functional involvement of Rab1A in microtubule-dependent anterograde melanosome transport in melanocytes. *J. Cell Sci.*, **125**: 5177–5187.
- Ishida, M., Marubashi, S., and Fukuda, M. 2017. M-INK, a novel tool for visualizing melanosomes and melanosomes. *J. Biochem.*, **161**: 323–326.
- Itoh, T., Satoh, M., Kanno, E., and Fukuda, M. 2006. Screening for target Rabs of TBC (Tre-2/Bub2/Cdc16) domain-containing proteins based on their Rab-binding activity. *Genes Cells*, **11**: 1023–1037.
- Kim, J.Y., Kim, J., Ahn, Y., Lee, E.J., Hwang, S., Almurayshid, A., Park, K., Chung, H.J., Kim, H.J., Lee, S.H., Lee, M.S., and Oh, S.H. 2019. Autophagy induction can regulate skin pigmentation by causing melanosome degradation in keratinocytes and melanocytes. *Pigment Cell Melanoma Res.*, doi: 10.1111/pcmr.12838.
- Kjos, I., Borg Distefano, M., Sætre, F., Repnik, U., Holland, P., Jones, A.T., Engedal, N., Simonsen, A., Bakke, O., and Progida, C. 2017. Rab7b modulates autophagic flux by interacting with Atg4B. *EMBO Rep.*, **18**: 1727–1739.
- Kobayashi, N., Nakagawa, A., Muramatsu, T., Yamashina, Y., Shirai, T., Hashimoto, M.W., Ishigaki, Y., Ohnishi, T., and Mori, T. 1998. Supranuclear melanin caps reduce ultraviolet induced DNA photoproducts in human epidermis. *J. Invest. Dermatol.*, **110**: 806–810.
- Matsui, T., Itoh, T., and Fukuda, M. 2011. Small GTPase Rab12 regulates constitutive degradation of transferrin receptor. *Traffic*, **12**: 1432–1443.
- Matsui, T. and Fukuda, M. 2013. Rab12 regulates mTORC1 activity and autophagy through controlling the degradation of amino-acid transporter PAT4. *EMBO Rep.*, **14**: 450–457.
- Morita, S., Kojima, T., and Kitamura, T. 2000. Plat-E: an efficient and stable system for transient packaging of retroviruses. *Gene Ther.*, **7**: 1063–1066.
- Mrozowska, P.S. and Fukuda, M. 2016. Regulation of podocalyxin trafficking by Rab small GTPases in 2D and 3D epithelial cell cultures. *J. Cell Biol.*, **213**: 355–369.
- Murase, D., Hachiya, A., Takano, K., Hicks, R., Visscher, M.O., Kitahara, T., Hase, T., Takema, Y., and Yoshimori, T. 2013. Autophagy has a significant role in determining skin color by regulating melanosome degradation in keratinocytes. *J. Invest. Dermatol.*, **133**: 2416–2424.
- Ohbayashi, N. and Fukuda, M. 2012. Role of Rab family GTPases and their effectors in melanosomal logistics. *J. Biochem.*, **151**: 343–351.
- Pfeffer, S.R. 2013. Rab GTPase regulation of membrane identity. *Curr. Opin. Cell Biol.*, **25**: 414–419.
- Progida, C., Cogli, L., Piro, F., De Luca, A., Bakke, O., and Bucci, C. 2010. Rab7b controls trafficking from endosomes to the TGN. *J. Cell Sci.*, **123**: 1480–1491.
- Progida, C., Nielsen, M.S., Koster, G., Bucci, C., and Bakke, O. 2012. Dynamics of Rab7b-dependent transport of sorting receptors. *Traffic*, **13**: 1273–1285.
- Raposo, G. and Marks, M.S. 2007. Melanosomes – dark organelles enlighten endosomal membrane transport. *Nat. Rev. Mol. Cell Biol.*, **8**: 786–797.
- Saitoh, T., Nakayama, M., Nakano, H., Yagita, H., Yamamoto, N., and Yamaoka, S. 2003. TWEAK induces NF- $\kappa$ B p100 processing and long lasting NF- $\kappa$ B activation. *J. Biol. Chem.*, **278**: 36005–36012.
- Seiberg, M., Paine, C., Sharlow, E., Andrade-Gordon, P., Costanzo, M., Eisinger, M., and Shapiro, S.S. 2000. The protease-activated receptor 2 regulates pigmentation via keratinocyte-melanocyte interactions. *Exp. Cell Res.*, **254**: 25–32.
- Serre, C., Busuttill, V., and Botto, J.M. 2018. Intrinsic and extrinsic regulation of human skin melanogenesis and pigmentation. *Int. J. Cosmet. Sci.*, **40**: 328–347.
- Spanò, S., Gao, X., Hannemann, S., Lara-Tejero, M., and Galán, J.E. 2016. A bacterial pathogen targets a host Rab-family GTPase defense pathway with a GAP. *Cell Host Microbe.*, **19**: 216–226.
- Stenmark, H. 2009. Rab GTPases as coordinators of vesicle traffic. *Nat. Rev. Mol. Cell Biol.*, **10**: 513–525.
- Tadokoro, R. and Takahashi, Y. 2017. Intercellular transfer of organelles during body pigmentation. *Curr. Opin. Genet. Dev.*, **45**: 132–138.
- Tamura, K., Ohbayashi, N., Maruta, Y., Kanno, E., Itoh, T., and Fukuda, M. 2009. Varp is a novel Rab32/38-binding protein that regulates Tyrp1 trafficking in melanocytes. *Mol. Biol. Cell*, **20**: 2900–2908.
- Tarafder, A.K., Bolasco, G., Correia, M.S., Pereira, F.J.C., Iannone, L., Hume, A.N., Kirkpatrick, N., Picardo, M., Torrisi, M.R., Rodrigues, I.P., Ramalho, J.S., Futter, C.E., Barral, D.C., and Seabra, M.C. 2014. Rab11b mediates melanin transfer between donor melanocytes and acceptor keratinocytes via coupled exo/endocytosis. *J. Invest. Derma-*

- tol.*, **134**: 1056–1066.
- Van Den Bossche, K., Naeyaert, J.M., and Lambert, J. 2006. The quest for the mechanism of melanin transfer. *Traffic*, **7**: 769–778.
- Wang, Y., Chen, T., Han, C., He, D., Liu, H., An, H., Cai, Z., and Cao, X. 2007. Lysosome-associated small Rab GTPase Rab7b negatively regulates TLR4 signaling in macrophages by promoting lysosomal degradation of TLR4. *Blood*, **110**: 962–971.
- Wu, X.S., Masedunskas, A., Weigert, R., Copeland, N.G., Jenkins, N.A., and Hammer, J.A. 2012. Melanoregulin regulates a shedding mechanism that drives melanosome transfer from melanocytes to keratinocytes. *Proc. Natl. Acad. Sci. USA*, **109**: E2101–E2109.
- Yang, M., Chen, T., Han, C., Li, N., Wan, T., and Cao, X. 2004. Rab7b, a novel lysosome-associated small GTPase, is involved in monocytic differentiation of human acute promyelocytic leukemia cells. *Biochem. Biophys. Res. Commun.*, **318**: 792–799.
- Yang, Z., Zeng, B., Pan, Y., Huang, P., and Wang, C. 2018. Autophagy participates in isoliquiritigenin-induced melanin degradation in human epidermal keratinocytes through PI3K/AKT/mTOR signaling. *Biomed. Pharmacother.*, **97**: 248–254.
- Yao, M., Liu, X., Li, D., Chen, T., Cai, Z., and Cao, X. 2009. Late endosome/lysosome-localized Rab7b suppresses TLR9-initiated proinflammatory cytokine and type I IFN production in macrophages. *J. Immunol.*, **183**: 1751–1758.
- Yokoyama, K., Kaji, H., He, J., Tanaka, C., Hazama, R., Kamigaki, T., Ku, Y., Tohyama, K., and Tohyama, Y. 2011. Rab27a negatively regulates phagocytosis by prolongation of the actin-coating stage around phagosomes. *J. Biol. Chem.*, **286**: 5375–5382.

(Received for publication, December 11, 2019, accepted, January 31, 2020 and published online, February 7, 2020)